

Finite Element Analysis of Steady-State Heat Conduction

Abstract

A numerical study was conducted to determine the steady-state temperature distribution in a square steel plate subjected to localized heat generation at its centre. The governing two-dimensional heat conduction equation was solved using the finite element method with linear triangular elements. Multiple mesh configurations were examined to investigate the influence of discretisation density on solution behaviour and numerical convergence. The heat source was modelled as a concentrated input using an equivalent nodal load representation consistent with a Dirac-delta formulation. Two boundary-condition scenarios were analysed: (i) insulated boundaries with a prescribed temperature along one edge, and (ii) convective heat transfer along the boundary. Temperature contours and centreline temperature variations were evaluated to compare solution characteristics across meshes and boundary conditions. Results demonstrate progressive smoothing and stabilization of the temperature field with mesh refinement and highlight the effect of convective heat removal on peak temperature levels and thermal gradients.

Problem Definition

A square plate of dimensions $1\text{ m} \times 1\text{ m}$ and thickness 0.01 m is subjected to steady heat conduction with internal heat generation applied at the geometric centre. The problem is treated as two-dimensional under the assumption of uniform temperature variation through the thickness.

The governing equation for steady heat conduction with internal heat generation is

$$-\nabla \cdot (k\nabla T) = q$$

where

T is temperature

k is thermal conductivity

q represents internal heat generation per unit area.

The heat input is modelled as a concentrated source located at the centre of the plate,

$$q = q_0 \delta(x - x_c, y - y_c)$$

where δ denotes the Dirac delta function and (x_c, y_c) is the plate centre.

Two boundary-condition cases were studied:

Case 1

Three edges of the plate are insulated, implying zero normal heat flux,

$$\frac{\partial T}{\partial n} = 0$$

(where n is the normal direction to that edge)

while the fourth edge is maintained at a constant temperature of 298 K.

Case 2

Three edges remain insulated, while the fourth edge is subjected to convective heat transfer governed by

$$q_n = h(T - T_0)$$

(where h is the convection coefficient and T_0 is the ambient temperature)

The objective of the study is to compute the temperature distribution, examine mesh refinement effects, and compare thermal behaviour under prescribed temperature and convective boundary conditions.

Finite Element Formulation

The governing heat conduction equation was solved using the finite element method based on a Galerkin weighted residual formulation. The computational domain was discretised into linear triangular elements, and the temperature field was approximated using interpolation functions defined over each element.

Weak Form

Starting from the steady-state heat conduction equation

$$-\nabla \cdot (k\nabla T) = q$$

a weighting function w is introduced and the equation is integrated over the domain Ω

$$\int_{\Omega} w (-\nabla \cdot (k\nabla T)) d\Omega = \int_{\Omega} wq d\Omega$$

Applying integration by parts reduces the order of differentiation and yields the weak form. Under the Galerkin approach, the weighting functions are chosen identical to the interpolation (shape) functions.

Element Discretisation

The temperature field within each triangular element is approximated as

$$T(x, y) = \sum_{i=1}^3 N_i(x, y) T_i$$

where N_i are linear shape functions and T_i are nodal temperatures.

Natural coordinates (ξ, η) are used to define interpolation functions

$$N_1 = \xi \quad N_2 = \eta \quad N_3 = 1 - \xi - \eta$$

These functions ensure linear variation of temperature within each element and continuity across element boundaries.

Coordinate Transformation

Integration over irregular triangular elements is performed using natural coordinates. Spatial derivatives are transformed using the Jacobian matrix.

$$\mathbf{J} = \begin{bmatrix} \frac{\partial x}{\partial \xi} & \frac{\partial y}{\partial \xi} \\ \frac{\partial x}{\partial \eta} & \frac{\partial y}{\partial \eta} \end{bmatrix}$$

Element Stiffness Matrix

Substituting the finite element approximation into the weak form yields the element-level equation

$$\mathbf{K}^{(e)} \mathbf{T}^{(e)} = \mathbf{F}^{(e)}$$

where the element stiffness matrix is

$$\mathbf{K}^{(e)} = \int_{\Omega_e} k (\nabla N)^T (\nabla N) d\Omega$$

and the load vector contains contributions from internal heat generation and boundary effects. Element matrices were evaluated through numerical integration in natural coordinates and subsequently assembled to form the global system of equations

Boundary Condition Implementation

Boundary conditions were incorporated into the finite element formulation through appropriate modifications to the global system of equations. Two types of boundary conditions were considered: prescribed temperature (Dirichlet), insulated boundaries (Neumann), and convective heat transfer (Robin condition).

Prescribed Temperature Boundary (Dirichlet Condition)

For Case 1, one edge of the plate was maintained at a fixed temperature of 298 K. This represents an essential boundary condition imposed directly on nodal temperatures.

After global assembly, the system of equations takes the form

$$\mathbf{KT} = \mathbf{F}$$

Nodes with known temperatures are separated from unknown degrees of freedom through matrix partitioning

$$\begin{bmatrix} K_{ff} & K_{fc} \\ K_{cf} & K_{cc} \end{bmatrix} \begin{bmatrix} T_f \\ T_c \end{bmatrix} = \begin{bmatrix} F_f \\ F_c \end{bmatrix}$$

where subscripts f and c denote free and constrained/fixed nodes respectively.

4.2 Insulated Boundaries (Neumann Condition)

The remaining three edges of the plate were assumed insulated, implying zero normal heat flux

$$q_n = -k \frac{\partial T}{\partial n} = 0$$

In the weak formulation, insulated boundaries contribute no additional terms to the system equations and are therefore satisfied naturally within the finite element formulation.

4.3 Convective Boundary Condition (Robin Condition)

In Case 2, the prescribed temperature boundary was replaced by convective heat transfer governed by

$$q_n = h(T - T_0)$$

where h is the convection coefficient and T_0 is the ambient temperature.

Substituting this relation into the boundary integral term of the weak form produces two additional contributions:

1. Boundary stiffness contribution

$$\int_{\Gamma} h N_i N_j d\Gamma$$

which modifies the global stiffness matrix.

2. Boundary load contribution

$$\int_{\Gamma} h T_0 N_i d\Gamma$$

which contributes to the global load vector.

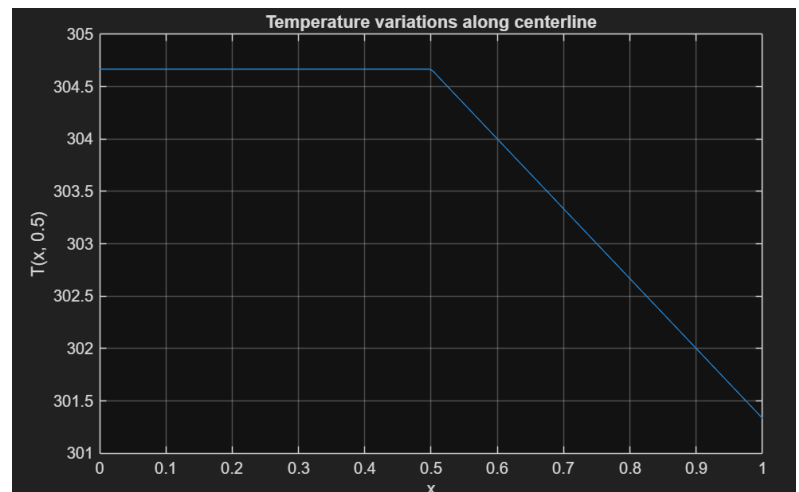
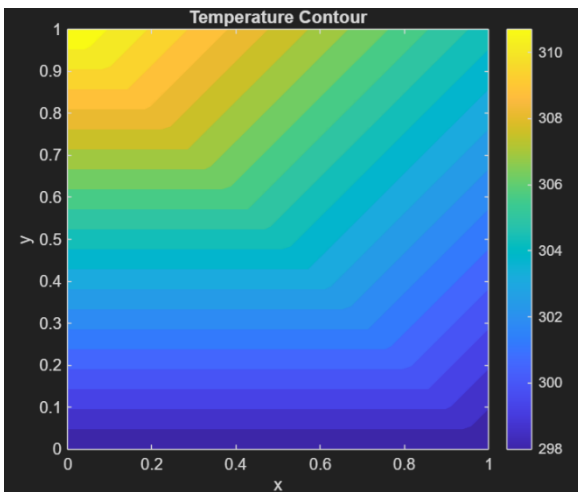
These terms were evaluated along boundary edges subjected to convection and assembled into the global matrices during element processing.

Results

The temperature distribution obtained from each mesh configuration was analysed using contour plots and temperature variation along a horizontal centreline passing through the plate centre. Comparisons were made to evaluate mesh refinement effects and the influence of boundary conditions on the thermal response.

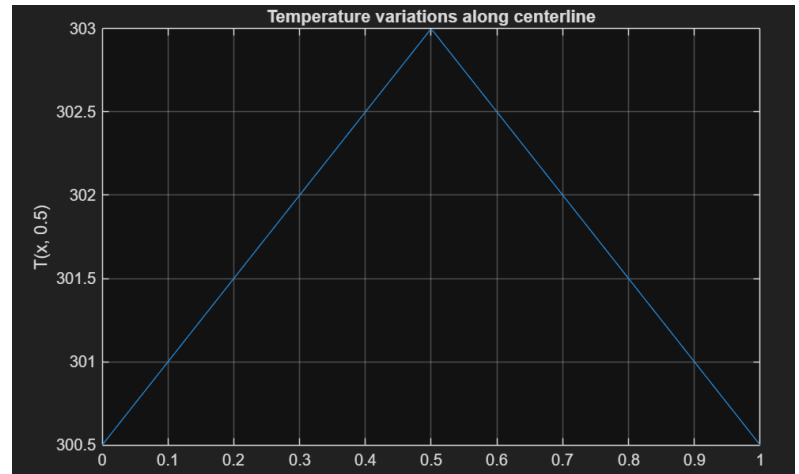
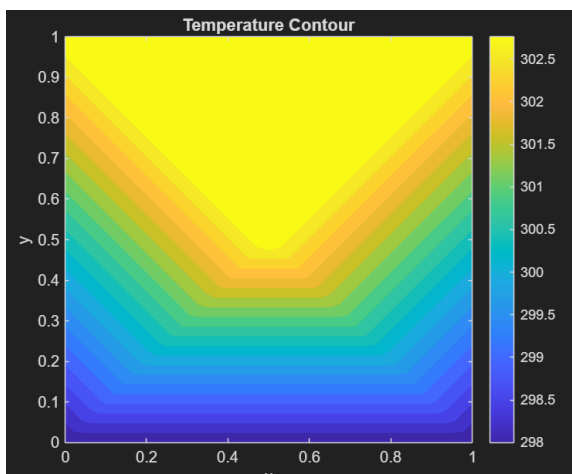
Case 1(a)

For the 2-element mesh, the temperature field exhibits large gradients within individual elements due to the coarse discretisation. The localized heat source cannot be adequately resolved, resulting in noticeable discontinuities in temperature variation across the domain.



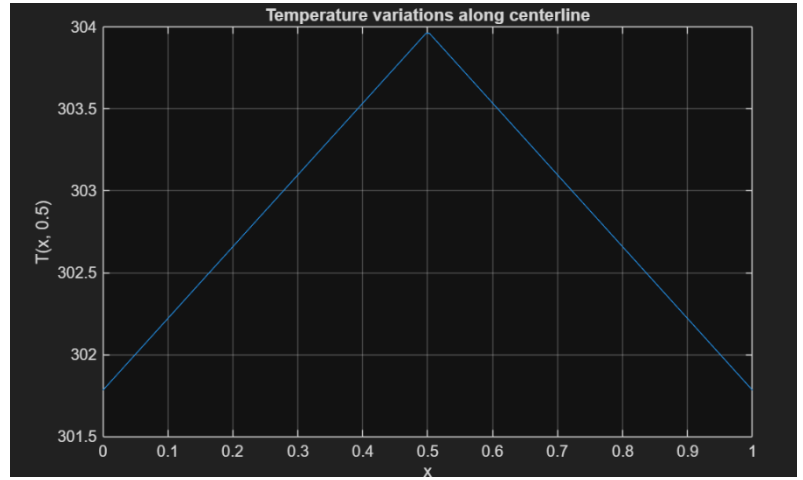
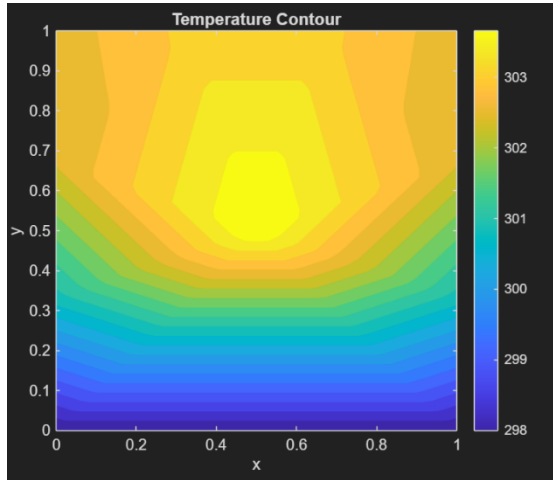
Case 1(b)

Introducing a central node in the 4-element mesh significantly improves symmetry of the solution. Because the heat source coincides with a node shared by all elements, the temperature field becomes more physically consistent and peak temperatures are distributed more uniformly.



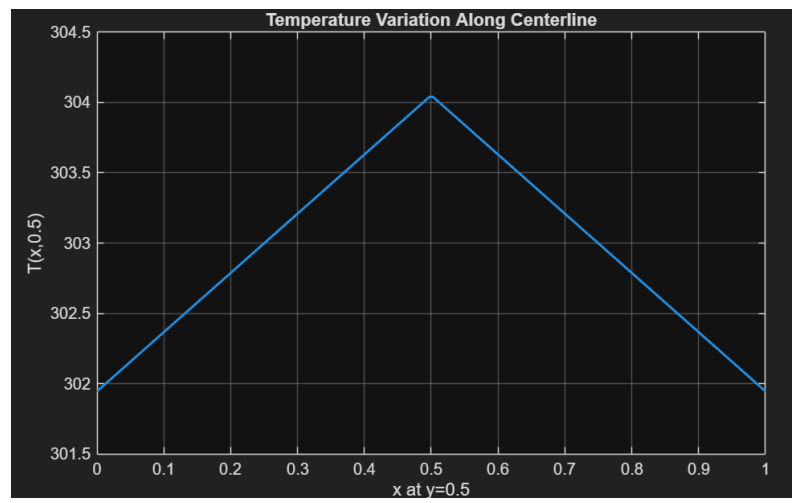
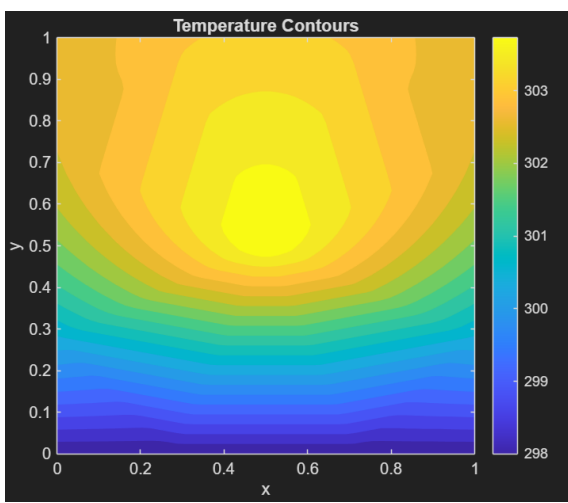
Case 1(c)

Further refinement produces smoother temperature contours and reduced variation between neighbouring nodal temperatures. The numerical solution begins to stabilize as additional elements allow improved representation of steep gradients near the heat source.



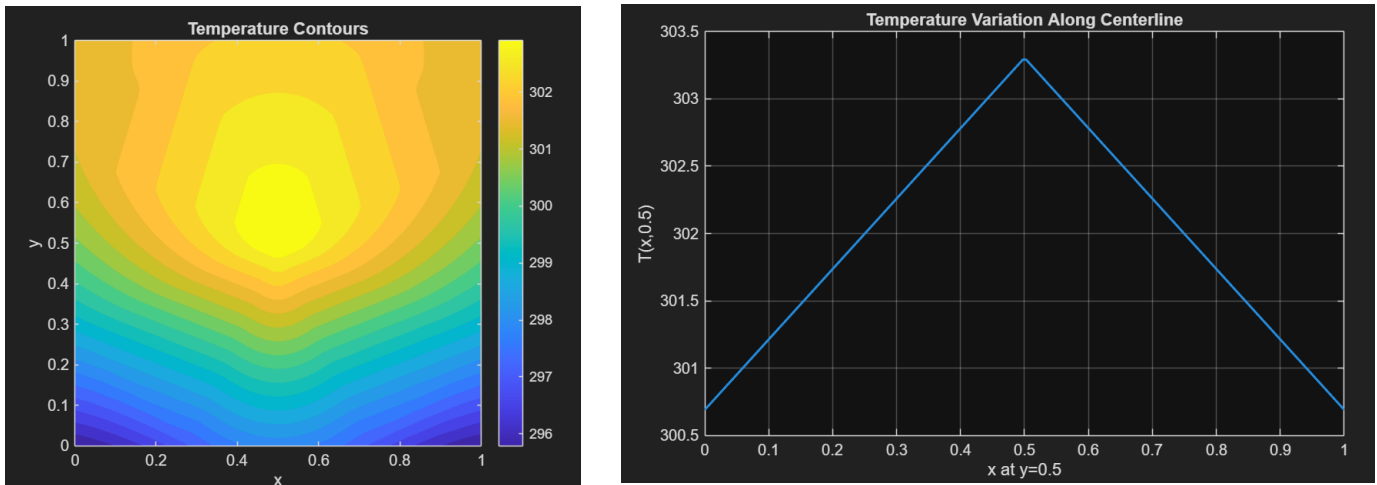
Case 1(d)

The 100-element mesh yields a smooth and continuous temperature distribution across the plate. Temperature contours become nearly symmetric about the plate centre, indicating that discretisation error has been substantially reduced. Differences between adjacent nodal temperatures decrease markedly, demonstrating convergence toward a mesh-independent solution.



Case 2

Unlike Case 1, where temperature is constrained at the boundary, convective heat transfer allows temperature to adjust based on heat exchange with the surroundings.



Conclusion

A finite element analysis was performed to determine the steady-state temperature distribution in a square plate subjected to localized heat generation at its centre. The study examined multiple mesh configurations and boundary-condition scenarios to evaluate numerical behaviour and physical response.

The following conclusions can be drawn:

1. The finite element formulation using linear triangular elements successfully captured the temperature field associated with a concentrated heat source when implemented through equivalent nodal loading.
2. Mesh refinement significantly improved solution quality, reducing artificial temperature gradients and producing smoother contour distributions consistent with physical expectations.
3. Placement of the heat source at a shared mesh node enhanced symmetry and stability of the numerical solution compared to coarse discretisation.
4. Increasing the number of elements led to convergence of both temperature contours and centreline temperature profiles, indicating reduction of discretisation error.
5. Replacing the prescribed temperature boundary with a convective boundary condition reduced peak temperatures and redistributed thermal gradients due to continuous heat exchange with the environment.